microbial biotechnology

Open Access

YALI0C22088g from *Yarrowia lipolytica* catalyses the conversion of L-methionine into volatile organic sulfur-containing compounds

Quan-Lu Zhao,† Zhu-Lin Wang,† Lan Yang, Sai Zhang and Kai-Zhi Jia*

Key Laboratory of Fermentation Engineering (Ministry of Education), Hubei Key Laboratory of Industrial Microbiology, Hubei Provincial Cooperative Innovation Center of Industrial Fermentation, Hubei University of Technology, Wuhan, 430068, China.

Summary

The enzymatic conversion of L-methionine (L-Met) into volatile organic sulfur-containing compounds (VOSCs) plays an important role in developing the characteristic aroma of foods. However, the mechanism for the direct conversion of L-Met into VOSCs is still unclear in yeast cells used to make food products. Here, we show that the transcription profile of YALI0C22088g from *Yarrowia lipolytica* correlates positively with L-Met addition. YALI0C22088g catalyses the γ-elimination of L-Met, directly converting L-Met into VOSCs. YALI0C22088g also exhibits strong C-S lysis activities towards L-cystathionine and the other sulfur-containing compounds and forms a distinct cystathionine-γ-lyase subgroup. We identified eight key amino acid residues in YALI0C22088g, and we inferred that the size of the tunnel and the charges carried by the entrance amino acid residue are the determinants for the enzymatic conversion of L-Met into VOSCs. These findings reveal the formation mechanism of VOSCs produced directly from L-Met via the demethiolation pathway in *Yarrowia lipolytica*, which provides a rationale for engineering the enzymatic conversion of L-Met into VOSCs and thus stimulates the enzymatic production of aroma compounds.

Introduction

The enzymatic conversion of L-methionine (L-Met) into volatile organic sulfur-containing compounds (VOSCs) plays an important role in developing the characteristic aroma of foods, including animal products such as yogurt and cheese, fruits, vegetables, and alcoholic beverages (Gonda *et al*., 2013; Martinez-Cuesta *et al*., 2013; Liu *et al*., 2017; Xu *et al*., 2018; Fischer and Steinhaus, 2020; Bonnaffoux *et al*., 2021). This phenomenon is because VOSCs possess low odour thresholds and characteristic notes for the human nose (Kagkli *et al*., 2006; Splivallo *et al*., 2011; Martinez-Cuesta *et al*., 2013; Perea-Sanz *et al*., 2019). The development of sequencing technology and improved bioinformatic tools have significantly advanced the discovery of enzymes with the potential to catalyse the conversion of L-Met into VOSCs (Hebert *et al*., 2011, 2013; McAuliffe *et al*., 2019; Mardones *et al*., 2020). The identification of these enzymes and the discovery of their catalytic mechanism will promote the understanding of the formation mechanism for the final aroma of fermented foods (Sales *et al*., 2018; Cadinanos *et al*., 2019).

Saccharomyces cerevisiae, *Kluyveromyces lactis* and *Yarrowia lipolytica*, which are generally recognized as safe (GRAS) for food production by the United States Food and Drug Administration, degrade L-Met into VOSCs via the Ehrlich and demethiolation pathways (Perpete *et al*., 2005; Kagkli *et al*., 2006; Cholet *et al*., 2008). The Ehrlich pathway includes the transamination of L-Met into α-keto-methylthiobutyric acid (KMBA), the decarboxylation of KMBA into methional, and reduction of methional to methionol (Hazelwood *et al*., 2008; Gonda *et al*., 2013; Martinez-Cuesta *et al*., 2013; Fischer and Steinhaus, 2020). Methionol presents a cooked-vegetable aroma in Chinese liquor and a cauliflower aroma in wine and beer (Landaud *et al*., 2008; Sha *et al*., 2017). Aminotransferases, decarboxylases and dehydrogenases that catalyse the three-step reactions in the Ehrlich pathway have been annotated based on homology (Splivallo *et al*., 2011; Hebert *et al*., 2011, 2013; Xu *et al*., 2018). In the demethiolation pathway, methionine-γ-lyase catalyses the demethiolation reaction, and L-Met is catabolized into methanethiol (MTL), after which MTL is rapidly oxidized to form dimethyl sulfide (DMS), dimethyl disulfide (DMDS) and dimethyl trisulfide (DMTS) via free radical reactions (Hazelwood *et al*., 2008; Martinez-Cuesta *et al*., 2013; Gonda *et al*., 2013; Fischer and Steinhaus, 2020). DMS exhibits an onion and cooked-

Received 9 December, 2020; revised 30 January, 2021; accepted 24 February, 2021.
*For correspondence. E-mail kaizhijia1@163.com; Tel.; Fax +86 027 59750483.
†These authors contributed equally to this work.
Microbial Biotechnology (2021) **14**(4), 1462–1471
doi:10.1111/1751-7915.13796

cabbage aroma in Chinese liquor and an onion aroma in wine and beer and can be used to mimic the aroma of the black Perigord truffle *Tuber melanosporum* (Fan and Qian, 2005; Landaud *et al*., 2008; Splivallo *et al*., 2011). Cystathionine γ-lyase catalyses the γ-elimination of L-Met (methionine γ-lyase) and degrades L-Met into α-ketobutyrate, MTL and NH_4^+ (Messerschmidt *et al*., 2003). While YAL012W (cystathionine-γ-lyase, EC 4.4.1.1, as encoded by *CYS3*) exhibited no activity towards L-Met, STR3 (cystathionine β-lyase, EC 4.4.1.8) from *S. cerevisiae* and its homologues in *Clonostachys rosea* isolated from *Tuber melanosporum* ascocarps showed no or negligible activity towards L-Met (Yamagata *et al*., 1993; Holt *et al*., 2012; Jia *et al*., 2016). It is therefore essential to elucidate the mechanism for the direct conversion of L-Met into VOSCs in the demethiolation pathway, which plays an important role in the formation of the final food aroma.

In this study, we used bioinformatic, biochemical and computational chemistry-based analyses to identify the yeast methionine γ-lyases and unravel their catalytic mechanism. Pyridoxa L-5′-phosphate (PLP)-dependent enzymes are involved in the metabolism of L-Met and the other sulfur-containing amino acids, and these enzymes form an evolutionarily related family, which were designated the L-Met metabolism PLP-dependent enzymes (Messerschmidt *et al*., 2003). We mined these enzymes from the genomes of *S. cerevisiae*, *K. lactis* and *Y. lipolytica* and then defined the function of methionine γ-lyase and the determinants for the enzymatic γ-elimination of L-Met. The results of this study promote an understanding of the formation mechanism for the final aroma of fermented foods and provide a rationale for the enzymatic production of aroma compounds.

Results and discussion

YHR112C, KLLA0_E21319g and YALI0C22088g are related to L-Met metabolism

Exogenous L-Met strongly induced the transcriptional expression of L-Met catabolism genes (Kagkli *et al*., 2006; Cholet *et al*., 2008; Jia *et al*., 2016; Xu *et al*., 2018). To mine the genes governing enzymatic L-Met depletion, 5 g l^{-1} L-Met was added to fermentation medium to induce the expression of L-Met depletion-related genes. After being cultured for 48 h, a 3 ml aliquot of liquid seed culture was sampled for yeast mRNA isolation. Through mRNA reverse transcription into cDNA and PCR cloning, 15 of 17 genes encoding proteins that contain the same motifs as the L-Met metabolism PLP-dependent enzyme were obtained (Fig. S1, Table S1). This result suggested that the 15 genes may be transcriptionally expressed in yeast cells. The 15 corresponding proteins fell into the 4 groups, namely cystathionine-β-lyase (EC 4.4.1.8), cystathionine-γ-lyase (EC 4.4.1.1), cystathionine-β-synthase (EC 4.2.1.22) and cystathionine-γ-synthase (EC 2.5.1.48) (Fig. 1A). Cystathionine γ-lyase catalyses the γ-elimination of L-Met, whereas YAL012W, which was named CYS3, exhibited no activity towards L-Met; STR3 from *C. rosea*, which is located in the cystathionine-β-lyase group, displayed negligible activity towards L-Met, and this conversion was attributed to the enzyme promiscuity of STR3 (Holt *et al*., 2012; Jia *et al*., 2016). Uncharacterized YHR112C, KLLA0_E21319g and YALI0C22088g clustered together and were separate from the abovementioned 4 groups, with YFR055W being annotated as a β-lyase (Fig. 1A). Expression of L-Met catabolic genes was shown to correlate positively with the conversion of L-Met into VOSCs (Bondar *et al*., 2005; Kagkli *et al*., 2006; Cholet *et al*., 2007; Hebert *et al*., 2011, 2013; Jia *et al*., 2016). In this study, the addition of 5 g l^{-1} L-Met induced increases in the mRNA abundances of YHR112C, KLLA0_E21319g and YALI0C22088g (Fig. 1B, Table S1), indicating that the transcriptional profiles of the 3 genes may be dependent on L-Met.

YALI0C22088g catalyses the γ-elimination of L-Met with high efficiency

YHR112C, KLLA0_E21319g and YALI0C22088g were heterologously expressed in *S. cerevisiae*, purified using Ni–nitrilotriacetic acid chromatography and identified (Fig. S2A–D). The purified proteins were incubated using L-Met as the substrate and pyridoxa L-5′-phosphate (PLP) as the cofactor. Sharp decreases in the L-Met concentration and the accumulation of α-ketobutyrate were observed for YALI0C22088g, while weak changes were observed for YHR112C (Fig. 1C, Fig. S3A-E, Fig. 2). This result is supported by the observation that *Y. lipolytica* produced a wider variety and quantity of VOSCs than *K. lactis* (Bondar *et al*., 2005; Cholet *et al*., 2007). The production of α-ketobutyrate did not correspond to the change in the L-Met concentration because α-ketobutyrate is not the direct product of L-Met (Fig. S3A, and B) and is unstable at pH 8.0 (the concentration of α-ketobutyrate decreased by 31.20% relative to that at pH 3.0). MTL is the direct product of L-Met and then rapidly oxidized to form DMS, DMDS, and DMTS via free radical reactions (Hazelwood *et al*., 2008; Gonda *et al*., 2013; Martinez-Cuesta *et al*., 2013; Fischer and Steinhaus, 2020). Therefore, MTL produced by YALI0C22088g catalysis was detected by reacting with 5,5'-dithiobis (2-nitrobenzoic acid) (DTNB). The activity of YALI0C22088g attained 239.96 ± 1.23 nmol MTL·min^{-1}·mg recombinant $protein^{-1}$, which approached the activity with the depletion of L-Met. These results indicated

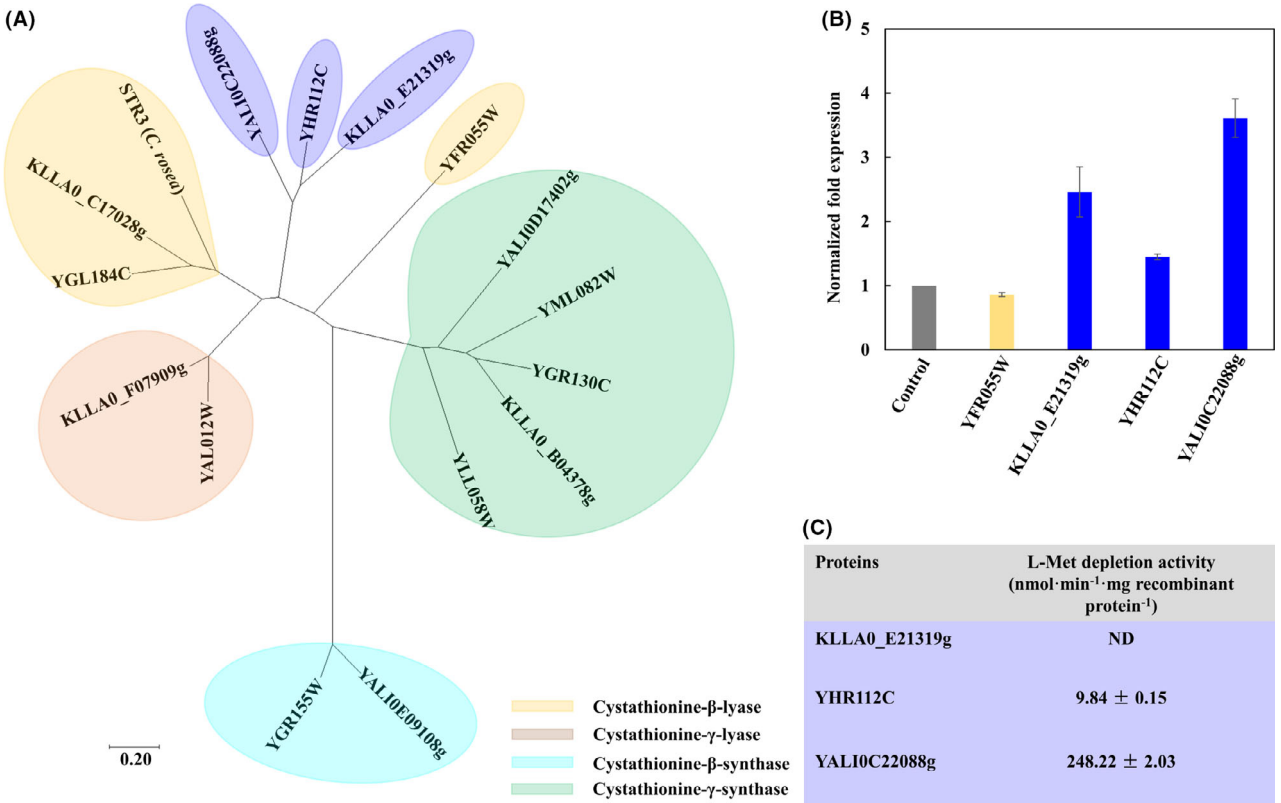

(C)

Proteins	L-Met depletion activity (nmol·min^{-1}·mg recombinant protein^{-1})
KLLA0_E21319g	ND
YHR112C	9.84 ± 0.15
YALI0C22088g	248.22 ± 2.03

Fig. 1. YALI0C22088g exhibited high catalytic capacity for L-Met depletion.
A. A non-rooted molecular phylogenetic tree of the enzymes related to L-Met metabolism. YGL184C (cystathionine β-lyase, EC 4.4.1.8, encoded by *STR3*) had no activity towards L-Met and clustered with STR3 (*C. rosea*), with negligible activity towards L-Met, and uncharacterized KLLA0_C17028g; the group was marked with yellow. YAL012W (cystathionine-γ-lyase, EC 4.4.1.1, encoded by *CYS3*) exhibiting no activity towards L-Met was clustered with uncharacterized KLLA0_F07909g, and the group was marked with brown. YGR155W (cystathionine β-synthase, EC 4.2.1.22, encoded by *CYS4*) was clustered with uncharacterized YALI0E09108g, and the group was marked with cyan. YML082W, YGR130C, YLL058W, KLLA0_B04378g and YALI0D17402g are uncharacterized and inferred to be cystathionine γ-synthases (EC 2.5.1.48) based on homology. YFR055W, functionally identified as a β-lyase (EC 4.4.1.13, encoded by *IRC7*), is far from the cystathionine-β-lyase group. Uncharacterized YHR112C, KLLA0_E21319g and YALI0C22088g are clustered together, and they deviated from the other groups.
B. The response of YHR112C, YFR055W, KLLA0_E21319g and YALI0C22088g to L-Met addition at the transcriptional level. L-Met addition upregulated the expression of YHR112C, KLLA0_E21319g and YALI0C22088g and downregulated the expression of YFR055W.
C. YALI0C22088g possessed a higher capacity for L-Met depletion than YHR112C. KLLA0_E21319g had no activity towards L-Met and was marked as not detected (ND).

that YALI0C22088g catalyses the γ-elimination of L-Met. In addition, YALI0C22088g exhibited a stronger catalytic activity towards L-Met than STR3 (*C. rosea*), which belongs to the cystathionine-β-lyase group (Table 1).

YALI0C22088g also catalysed the conversion of KMBA and methional into MTL (Table 2, Fig. 2). This result indicated that YALI0C22088g may function as a bridge between the demethiolation and Ehrlich pathways in *Y. lipolytica*. The identification of YALI0C22088g with C-S lysis activity enhances our understanding of the formation mechanism underlying the final fermented food aroma. YALI0C22088g possessed high substrate promiscuity and catalysed the depletion of L-cystathionine (L-cystathionine was converted into L-cysteine (Fig. S4A–C), and the same catalytic activity was observed for cystathionine-γ-lyase (Bruinenberg *et al.*, 1997) and L-homocysteine but not L-cystine and L-cysteine (Table 2, Fig. S5A and B), indicating that YALI0C22088g was a cystathionine γ-lyase. YALI0C22088g shared 27.1% and 30.6% identities with cystathionine-γ-lyases 3VK3 and 5TSU (Fukumoto *et al.*, 2012; Yan *et al.*, 2017) having the ability to degrade L-Met, and is categorized apart from the cystathionine -γ-lyase group. Thus, YALI0C22088g forms a distinct subgroup of cystathionine-γ-lyase (Fig. S6). Methionine-γ-lyase, which catalyses L-Met depletion, is one of the most promising enzymes for cancer therapy (Sun *et al.*, 2003). 3VK3 from *Pseudomonas putida* retarded tumour growth, but it was highly immunogenic in primates (Fukumoto *et al.*, 2012; Stone *et al.*, 2012). YALI0C22088g was from *Y. lipolytica* verified to be GRAS and inferred to be with low immunogenic potential. YALI0C22088g displayed higher L-Met binding ability than 5TSU (K_m = 14 ± 1.5 mM) (Stone *et al.*, 2012) (Table 1), and

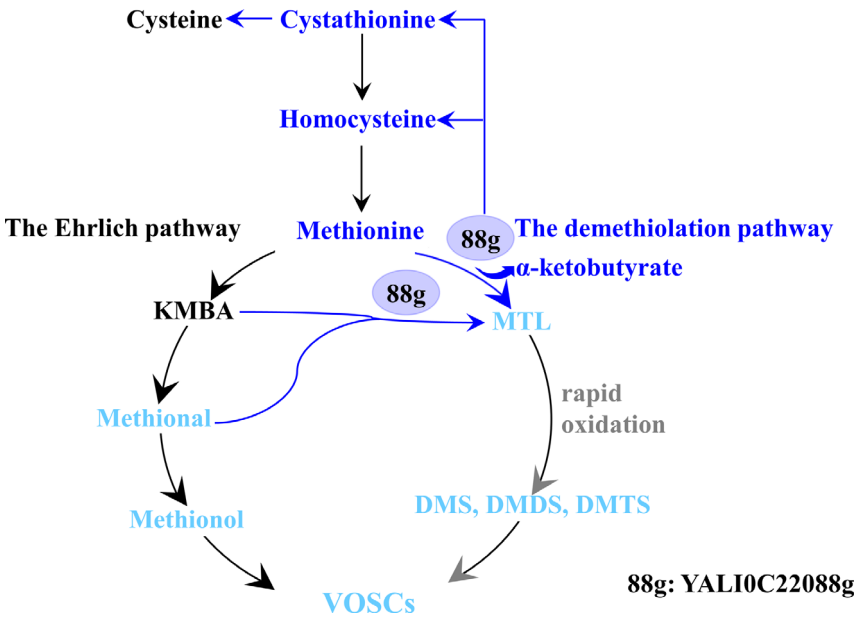

Fig. 2. YALI0C22088g exhibited strong C-S lysis activity towards L-Met and its precursors and catabolic products. YALI0C22088g catalysed the production of α-ketobutyrate and MTL and was identified as a methionine-γ-lyase. It also exhibited strong C-S lysis activities towards L-cystathionine, L-homocysteine, KMBA and methional.

Table 1. γ-elimination activity towards L-Met.

	K_m (mM)	V_{max} (mM min^{-1})	k_{cat} (s^{-1})	k_{cat}/K_m (M^{-1} s^{-1})
YALI0C22088g	3.33 ± 0.17	0.16 ± 0.01	0.19 ± 0.01	57.06
YALI0C22088g (Y59A)	0.62 ± 0.05	0.06 ± 0.00	0.07 ± 0.00	112.90
STR3 (*C. rosea*) (Jia *et al.*, 2016)	196.37	0.034 μM min^{-1}		

further engineering of YALI0C22088g will improve its application in cancer therapy.

Key elements determining the conversion of L-Met into VOSCs in YALI0C22088g

To locate the key amino acid residues that determine the high L-Met depletion activity of YALI0C22088g, we compared the amino acid sequence of YALI0C22088g to those of YHR112C and KLLA0_E21319g, which share 54.40% and 54.79% of their identities with YALI0C22088g, respectively, in according with the methods described by Jia *et al.* (2019). Twelve out of 29 amino acid residues constituting the entrance, tunnel and active site in YALI0C22088g were different from those in YHR112C and KLLA0_E21319g (Fig. 3A and B). The 12 amino acid residues were individually mutated to Ala by using alanine scanning mutagenesis (Weiss, *et al.*, 2000; Pal, *et al.*, 2005; Sidhu and Kossiakoff, 2007), and then, the L-Met depletion activities of these mutants were analysed. The P239A mutant was inactive, and the S70A, K74A, N89A, S237A, G238A and G240A mutants exhibited lower L-Met depletion activity (below 20% relative activity), while the Y59A mutant displayed 0.28-fold increased activity compared with that of wild-type YALI0C22088g, indicating that the 8 amino acid residues are essential for L-Met depletion (Fig. 4A). By positioning the 8 amino acid residues in the predicted 3D structure of YALI0C22088g, we found that Y59, S70 and K74 were located in the entrance and that N89, S237, G238, P239 and G240 were located in the tunnel (Fig. 4B, Fig. 5A–C). The mutant Y59A increased the bottleneck radius of YALI0C22088g from 1.5 Å to 2.0 Å (Fig. 4C), which may result in the enlargement of the tunnel size and enable more substrate to enter the active site. This inference was supported by the observation that the L-Met binding ability and catalytic efficiency of mutant Y59A were increased by 4.37- and 0.98-fold relative to those of YALI0C22088g (Table 1). The tunnel was not detected for the mutant S70A (Fig. 4C); thus, its lower L-Met depletion activity was attributed to the destruction of the tunnel. L-Met carries a negative charge (the pI of L-Met is 5.75, and the buffer pH was 8.0), the mutant K74A

Table 2. Substrate specificity of purified YALI0C22088g.

	Substrates	Structural formula	Conversion (%)
1	L-Met	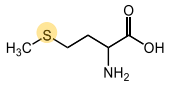	30
2	KMBA	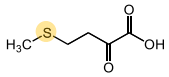	16
3	Methional	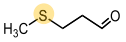	8
4	Methionol	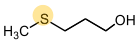	ND
5	L-cystathionine	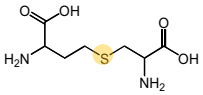	44
6	L-homocysteine	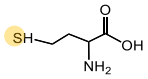	97
7	L-cystine	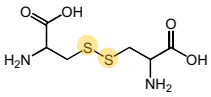	ND
8	L-cysteine	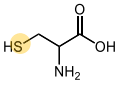	ND

ND, not detected. C-S lysis activities with different substrates were determined in the standard enzyme assay system. The conversion rates of L-Met, L-cystathionine, L-homocysteine, L-cystine and L-cysteine were calculated by measuring the molar concentration ratios of the depleted and initial substrates. The conversion rates of MTL from KMBA, methional and methionol were calculated by measuring the molar concentration ratio of MTL to the initial substrates. MTL and its derivatives were not detected by GC-MS using methionol as the substrate according to the method described by Jia *et al.* (2016).

eliminated the positive charge (Fig. 4C, Fig. S7A, Table S2), and its lower L-Met depletion activity was inferred to be related to the abolishment of the charge attraction effect between K74 and L-Met, which enabled L-Met to enter the active site more easily.

Conclusion

We identified YALI0C22088g from *Y. lipolytica* as a methionine γ-lyase and defined the determinants of the enzymatic γ-elimination of L-Met. YALI0C22088g forms a distinct subgroup of cystathionine-γ-lyase, and it exhibited strong C-S lysis activities towards L-cystathionine, L-homocysteine, KMBA and methional (Fig. 2). We identified eight key amino acid residues in YALI0C22088g and found that the size of the tunnel and the charges carried by the entrance amino acid residues play important roles in the enzymatic conversion of L-Met into VOSCs (Fig. 4B). These findings reveal the formation mechanism of VOSCs produced through the demethiolation pathway, provide a rationale for engineering the enzymatic conversion of L-Met into VOSCs and thus promote the enzymatic production of aroma compounds.

Experimental procedures

Chemicals, strains, and culture conditions

Chemicals 1–8 (Table 2) were purchased from Sigma-Aldrich (St. Louis, MO, USA), the acetonitrile purchased from Fisher Scientific (USA) was of HPLC grade, and the other chemicals and reagents were purchased from Sigma-Aldrich, Tokyo Chemical Industry Co., Ltd. (Tokyo, Japan) and China National Pharmaceutical Group Corporation (Beijing, China). Competent cells, including *E. coli* BL21 (DE3) and *S. cerevisiae* INVSc1, were purchased from TransGen Biotech (Beijing, China) and Invitrogen (USA) and transformed according to the manufacturer's protocol. To analyse the gene expression at the transcriptional level, *S. cerevisiae* S288C and *K. lactis* NRRL Y-1140 were cultivated in synthetic complete medium containing 2% glucose, 0.67% yeast nitrogen base without amino acids (Biosharp) and 0.5% amino acids. *Y. lipolytica* CLIB122 was cultivated in potato dextrose broth and a defined synthetic medium according to the method described by Mansour *et al.* (2008). Then, 5 g l^{-1} L-Met was added into the medium to induce the expression of genes related to L-Met catabolism (Jia *et al.*, 2016; Xu *et al.*, 2018).

Gene cloning

The total RNA was isolated from *S. cerevisiae, K. lactis and Y. lipolytica* using a Total RNA Kit II R6934 (Omega Bio-tek, USA) and then reverse transcribed into complementary DNA (cDNA) using a SMARTer™ PCR cDNA Synthesis Kit (Clontech, USA). The cDNA was used as the template for amplifying the genes YHR112C, YFR055W, YGL184C, YGR155W, YLL058W, YML082W, YGR130C and YAL012W (*S. cerevisiae*); KLLA0_C17028g, KLLA0_F07909g, KLLA0_B04378g, KLLA0_F09317g and KLLA0_E09108g (*K. lactis*); and YALI0E09108g, YALI0C22088g, YALI0F05874g and YALI0D17402g (*Y. lipolytica*) because the corresponding enzymes possess the same motifs as the L-Met metabolism PLP-dependent enzyme (https://www.kegg.jp/kegg/catalog/org_list.html) (Table S1). Subsequently, the amplified fragments were sequenced and verified.

Phylogenetic analysis

The sequences of the proteins corresponding to the genes mentioned above were aligned and compared by using the multiple sequence alignment software

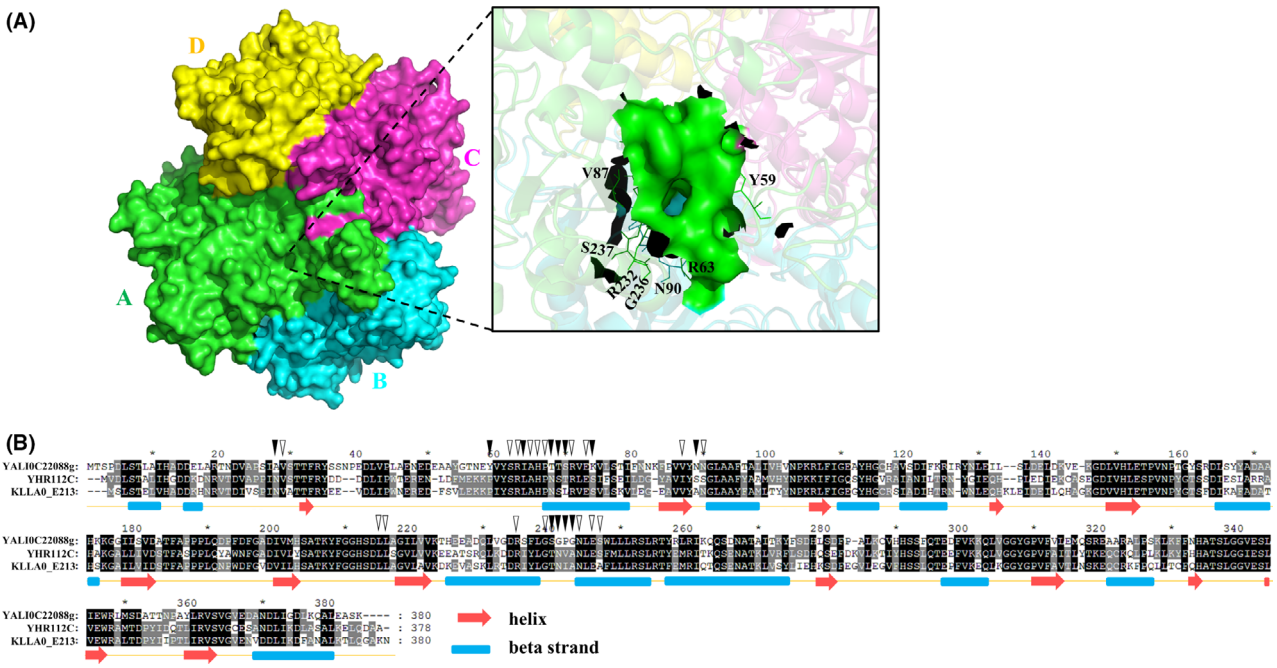

Fig. 3. Inferred essential amino acid residues in YALI0C22088g.
A. Residues constituting the entrance, tunnel and active site of YALI0C22088g. The model of YALI0C22088g was constructed using 5eig.1.A (PDB ID) as a template. The inferred amino acid residues are marked as line models, and their colours coincide with the corresponding monomers.
B. Amino acid sequence alignment of YALI0C22088g, YHR112 and KLLA0_E21319g. ClustalW was used to perform the alignment, and the numbering is given for YALI0C22088g. The predicted secondary structure elements of YALI0C22088g are shown. The entrance, tunnel and active site of YALI0C22088g were predicted with CAVER software, and the amino acid residues from the entrance, tunnel and active site in YALI0C22088g that differed from those in YHR112C and KLLA0_E21319g are indicated by solid triangular wedges and coincide with hollow triangular wedges.

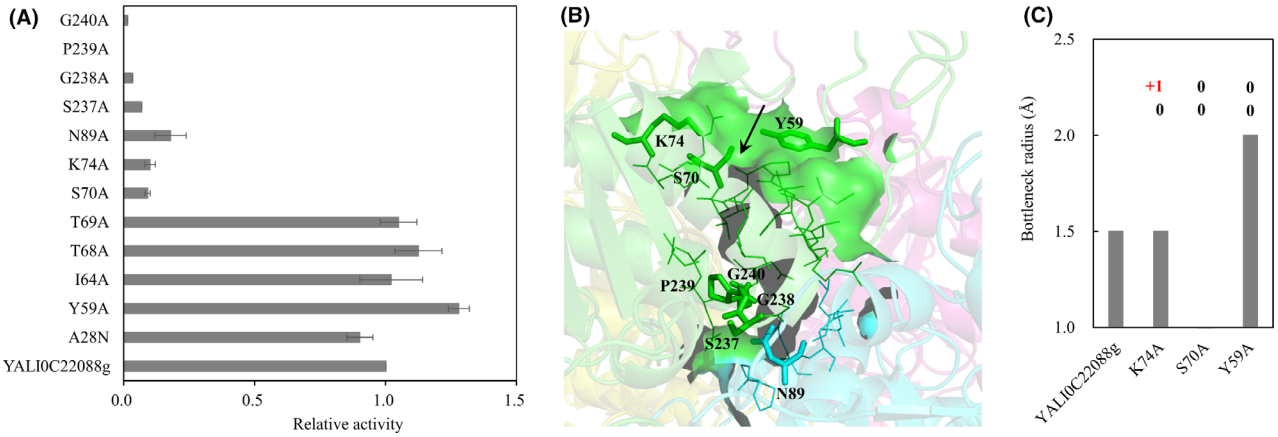

Fig. 4. Essential amino acid residues involved in L-Met depletion in YALI0C22088g.
A. Relative activity of purified YALI0C22088g and its mutants towards L-Met.B. The essential amino acid residues positioning in the YALI0C22088g model. Y59, S70 and K74 surround the putative entrance, the essential amino acid residues are marked as stick models, and their colours coincide with the corresponding monomers.
C. Analysis of bottleneck radius and electric charges for YALI0C22088g and its mutants Y59A, S70A and K74A. K74 carrying the positive charge in YALI0C22088g is marked in red (Fig. S7A), and the amino acids without charges is marked with 0.

ClustalW, and then, a phylogenetic tree was constructed from the ClustalW multiple sequence alignment using the neighbour-joining method in MEGA X 10.0.4. The bar = 0.2 amino acid substitutions/site.

Gene expression analysis

To examine the differential expression of YFR055W, KLLA0_E21319g, YHR112C and YALI0C22088g in

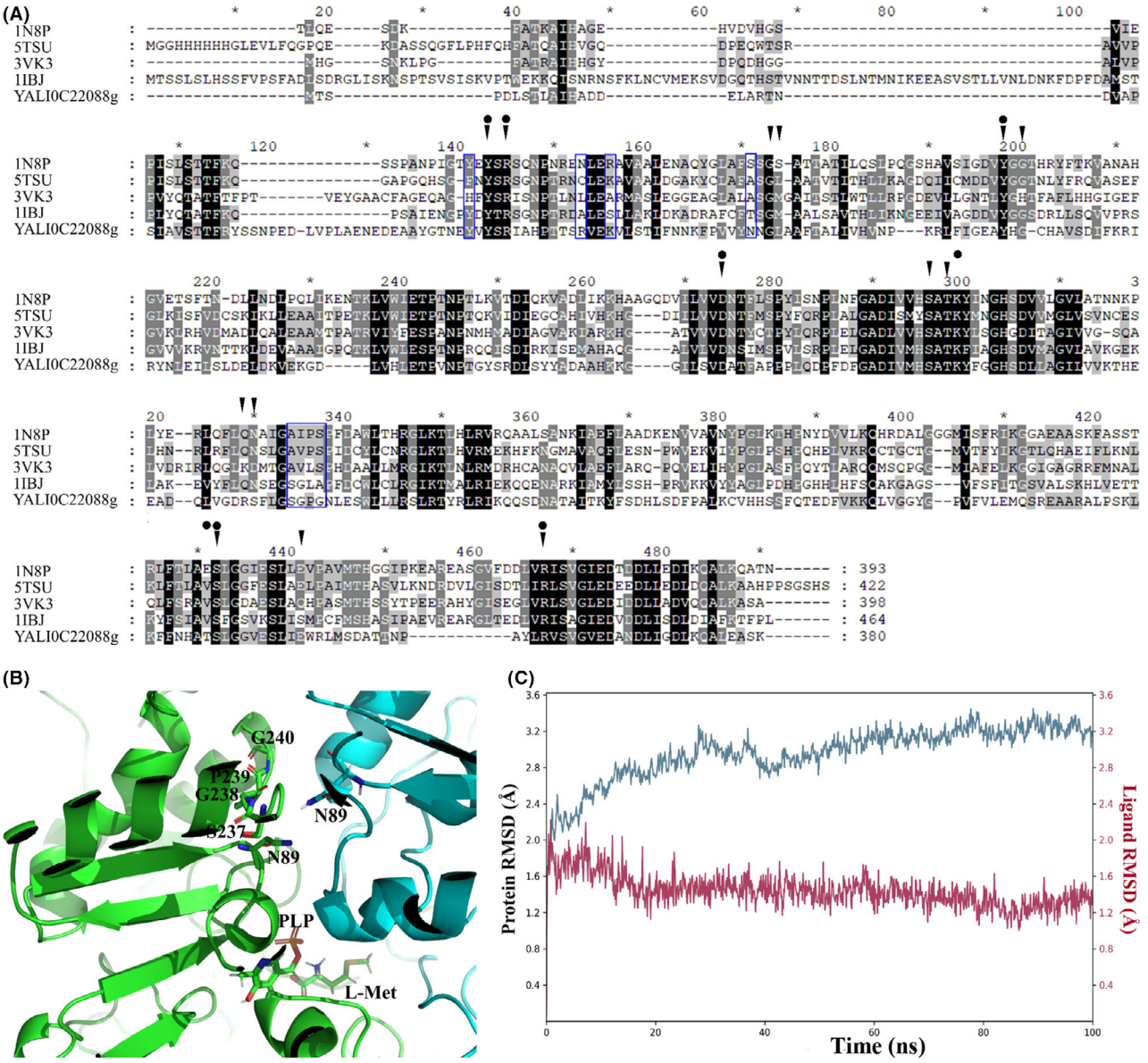

Fig. 5. Inferred functions of N89, S237, G238, P239 and G240.
A. Sequence alignment of YALI0C22088g with PLP-dependent enzymes. Numbering is given for 1IBJ, solid triangular wedges show 3VK3 (PDB ID, mutant methionine-γ-lyase from *Pseudomonas putida* C116) active site residues, solid circles show 1N8P (PDB ID, cystathionine γ-lyase from yeast) active site residues, and 1IBJ (PDB ID) is a cystathionine-β-lyase from *Arabidopsis*. 5TSU (PDB ID) is an engineered cystathionine-γ-lyase that acquired the ability to degrade L-Met. The 8 key amino acid residues boxed in blue in YALI0C22088g do not overlap with the active site residues of 3VK3 and 1N8P.
B. Structural model of YALI0C22088g with L-Met and PLP. N89, S237, G238, P239 and G240 are predicted to constitute the tunnel, and they are marked with stick models (Fig. S7B).
C. The time dependence of the root mean square deviations (RMSD) for YALI0C22088g (protein RMSD, marked in blue) and L-Met (ligand RMSD, marked in red).

response to L-Met addition, we designed primers for quantitative real-time PCR to detect and quantify the gene expression (Table S1). RNA was isolated from cells harvested from 2-day-old fermentation cultures and then reverse transcribed into cDNA by using the method mentioned above. Quantitative real-time PCR was performed in triplicate on a BIO-RAD CFX Connect™ (BIO-RAD). Power SYBR Green PCR Master Mix (Applied Biosystems cat: 4367659) was used to visualize the gene amplification. 18S rRNA was used as a housekeeping gene to normalize the expression of the genes related to L-Met depletion (Table S1). The comparative cycle threshold (C_T) method was adopted to evaluate the relative quantification of the target gene transcripts.

The mean values ± SD of three independent experiments are shown.

Heterologous expression and purification of enzymes related to L-Met metabolism

wThe full-length nucleic acid sequences of KLLA0_E21319g, YHR112C and YALI0C22088g were amplified and cloned into the yeast expression plasmid pYES2 (Table S1). To purify of these enzymes, a His-tag-encoding fragment was inserted after the second codon TCT. After the resulting plasmids were transformed into *S. cerevisiae* strain INVSc1, the enzymes, including KLLA0_E21319g, YHR112C and YALI0C22088g, were induced with galactose and purified by nickel affinity chromatography as described (Jia *et al.*, 2016). The concentrations of the purified proteins were determined using a BCA Protein Quantification Kit (Yeasen Biotech Co., Ltd., Shanghai, China). All the enzymes mentioned above were subjected to MALDI-TOF/TOF analysis.

C-S lysis activity determination

The L-Met depletion activity was assayed (in a total volume of 1 ml) in 50 mM Tris–HCl (pH 8.0, the optimal pH) containing 20 mM L-Met, 5 μM PLP and 0.6 mg of the purified enzymes. The reaction was performed at 30°C for 1 h. The complete assay with the inactivated enzymes (when boiled for 10 min) was used as a control experiment. The mean values ± SD of three independent experiments are shown. The decrease in the L-Met concentration and the production of α-ketobutyrate were detected by HPLC (Dionex UltiMate 3000; Thermo, Waltham, MA, USA). A 200 μl enzymatic reaction mixture was mixed with an equal amount of acetonitrile and then subjected to chromatographic separation on a Reprosil-Pur Basic C18 column (4.6 mm × 250 mm × 5 μm) from Dr Maisch GmbH (Germany) with 13%/87% acetonitrile/water adjusted to pH 3.0 by H_3PO_4 as the mobile phase and 230 nm as the detection wavelength. The column oven temperature and flow rate were 40°C and 0.5 ml min^{-1} respectively. The retention times for L-Met and α-ketobutyrate were 5.08 and 5.81 min respectively. Subsequently, the enzymatic conversion of L-Met into α-ketobutyrate was identified by an Ultimate 3000 UHPLC system coupled with a Q Exactive Focus mass spectrometer (Thermo Fisher Scientific, Waltham, MA, USA). The production of MTL was estimated by detecting the reaction of MTL with DTNB following a method described previously (Yamagata *et al.*, 1993). Decreases in the concentrations of L-cystathionine, L-homocysteine, L-cystine and L-cysteine were determined with an Ultimate 3000 UHPLC system coupled with a Q Exactive Focus mass spectrometer.

Generating YALI0C22088g mutants

To generate YALI0C22088g mutants, YALI0C22088g was synthesized and cloned into pET28a with GenScript (Nanjing, China), and the expressed YALI0C22088g was purified by nickel affinity chromatography. To identify the essential amino acid residues in YALI0C22088g, a Mut Express II Fast Mutagenesis Kit V2 (Vazyme, Nanjing, Jiangsu Province, China) was applied to mutate the selected amino acid residues to A (A28 of YALI0C22088g was mutated into the corresponding amino acid residue N25 of KLLA0_E21319g) by using the primers detailed in Table S1.

The L-Met concentrations used here were 0.1 to 10 mM with PLP at 5 μM for L-Met depletion kinetics, and the kinetic parameters were calculated following the method described by Asada *et al.* (2013). The total volume for the enzymatic reaction was 0.5 ml, and 0.3 mg of the purified enzymes was added into the reaction mixture. The reaction was performed at 30°C for 30 min. The decrease in the L-Met concentration was detected using the method described above. The data are shown as the mean values ± SD of three independent experiments.

Molecular model, molecular docking and molecular dynamics simulation

The model for YALI0C22088g was established by using SWISS-MODEL (https://swissmodel.expasy.org/). 5eig.1.A, carrying 35.5% sequential identity with YALI0C22088g, has the highest global model quality estimation (GMQE) value and was adopted as the template for building the 3D structure of YALI0C22088g. The entrances were predicted by CAVER software (https://loschmidt.chemi.muni.cz/hotspotwizard/) and displayed using PyMOL software (https://pymol.org/2/) (Mura *et al.*, 2010; Sumbalova *et al.*, 2018). The charge analysis was predicted by using PDB2PQR software (http://server.poissonboltzmann.org/opal-jobs) (Dolinsky *et al.*, 2004). We used Auto Dock Tools (ADT) from AutoDock 4.2 software for molecular docking. To obtain the conformations of PLP and L-Met in YALI0C22088g, we referred to the structures of 1N8P and 5TSU (PDB IDs) containing PLP and L-Met respectively. A molecular dynamics (MD) simulation of YALI0C22088g complexed with PLP and L-Met was performed using the Desmond module in the Schrodinger software package. The structure was immersed in a solvent box that extended 10 Å away from the solute border, and Na^+ or Cl^- ions were added into the box to neutralize the whole system. After energy minimization, the temperature and pressure of the system were set to 300 K and 1.01325 bar respectively. The SHAKE algorithm was applied to constrain all

of the bonds involving hydrogen atoms. A 2 fs integration step was used, and the total simulation time was 100 ns. The MD simulation was performed under the OPLS-2005 force field.

Acknowledgements

The authors are grateful to Prof. Xu-Dong Qu (Key Laboratory of Combinatorial Biosynthesis and Drug Discovery, Ministry of Education, School of Pharmaceutical Sciences, Wuhan University) for providing assistance in identifying key amino acid residues in the methionine-γ-lyases and to Jing Zhao (State Key Laboratory of Biocatalysis and Enzyme Engineering, Hubei University) for providing assistance with the charge analysis of the methionine-γ-lyases.

Funding Information

This work was supported by the National Natural Science Foundation of China (Grant Nos. 31570054 and 21838002).

Conflict of interest

The authors declare no conflicts of interest.

Author contributions

Kai-Zhi Jia designed the research and wrote the manuscript. Quan-Lu Zhao, Zhu-Lin Wang, Lan Yang and Sai Zhang performed the experiments. Kai-Zhi Jia, Quan-Lu Zhao and Zhu-Lin Wang analysed the data.

References

Asada, K., Salim, V., Masada-Atsumi, S., Edmunds, E., Nagatoshi, M., Terasaka, K., *et al*. (2013) A 7-deoxyloganetic acid glucosyltransferase contributes a key step in secologanin biosynthesis in *Madagascar Periwinkle*. *Plant Cell* **25:** 4123–4134.

Bondar, D.C., Beckerich, J.M., and Bonnarme, P. (2005) Involvement of a branched-chain aminotransferase in production of volatile sulfur compounds in *Yarrowia lipolytica*. *Appl Environ Microbiol* **71:** 4585–4591.

Bonnaffoux, H., Roland, A., Schneider, R., and Cavelier, F. (2021) Spotlight on release mechanism of volatile thiols in beverages. *Food Chem* **339:** 127628.

Bruinenberg, P.G., Roo, G.D., and Limsowtin, G.K.Y. (1997) Purification and characterization of cystathionine (gamma)-lyase from *Lactococcus lactis* subsp. cremoris SK11: possible role in flavor compound formation during cheese maturation. *Appl Environ Microbiol* **63:** 561–566.

Cadinanos, L.P., Garcia-Cayuela, T., Martinez-Cuesta, M.C., Pelaez, C., and Requena, T. (2019) Expression of amino acid converting enzymes and production of volatile compounds by *Lactococcus lactis* IFPL953. *Int Dairy J* **96:** 29–35.

Cholet, O., Hénaut, A., Casaregola, S., and Bonnarme, P. (2007) Gene expression and biochemical analysis of cheese-ripening yeasts: focus on catabolism of L-methionine, lactate, and lactose. *Appl Environ Microbiol* **73:** 2561–2570.

Cholet, O., Henaut, A., Hebert, A., and Bonnarme, P. (2008) Transcriptional analysis of L-methionine catabolism in the cheese-ripening yeast *Yarrowia lipolytica* in relation to volatile sulfur compound biosynthesis. *Appl Environ Microbiol* **74:** 3356–3367.

Dolinsky, T.J., Nielsen, J.E., McCammon, J.A., and Baker, N.A. (2004) PDB2PQR: an automated pipeline for the setup, execution, and analysis of Poisson-Boltzmann electrostatics calculations. *Nucleic Acids Res* **32:** W665–W667.

Fan, W.L., and Qian, M.C. (2005) Headspace solid phase microextraction and gas chromatography-olfactometry dilution analysis of young and aged Chinese "Yanghe Daqu" liquors. *J Agric Food Chem* **53:** 7931–7938.

Fischer, N.S., and Steinhaus, M. (2020) Identification of an important odorant precursor in durian: first evidence of ethionine in plants. *J Agric Food Chem* **68:** 10397–10402.

Fukumoto, M., Kudou, D., Murano, S., Shiba, T., Sato, D., Tamura, T., *et al*. (2012) The role of amino acid residues in the active site of L-methionine gamma-lyase from *Pseudomonas putida*. *Biosci Biotech Bioch* **76:** 1275–1284.

Gonda, I., Lev, S., Bar, E., Sikron, N., Portnoy, V., Davidovich-Rikanati, R., *et al*. (2013) Catabolism of L-methionine in the formation of sulfur and other volatiles in melon (*Cucumis melo* L.) fruit. *Plant J* **74:** 458–472.

Hazelwood, L.A., Daran, J.M., Maris, A.J., Pronk, J.T., and Dickinson, J.R. (2008) The Ehrlich pathway for fusel alcohol production: a century of research on *Saccharomyces cerevisiae* metabolism. *Appl Environ Microbiol* **74:** 2259–2266.

Hebert, A., Forquin-Gomez, M.P., Roux, A., Aubert, J., Junot, C., Loux, V., *et al*. (2011) Exploration of sulfur metabolism in the yeast *Kluyveromyces lactis*. *Appl Microbiol Biotechnol* **91:** 1409–1423.

Hebert, A., Forquin-Gomez, M.P., Roux, A., Aubert, J., Junot, C., Heilier, J.F., *et al*. (2013) New insights into sulfur metabolism in yeasts as revealed by studies of *Yarrowia lipolytica*. *Appl Environ Microbiol* **79:** 1200–1211.

Holt, S., Cordente, A.G., and Curtin, C. (2012) *Saccharomyces cerevisiae* STR3 and yeast cystathionine β-lyase enzymes. *Bioeng Bugs* **3:** 178–180.

Jia, K.Z., Zhang, Q., Sun, L.Y., Xu, Y.H., Li, H.M., and Tang, Y.J. (2016) *Clonostachys rosea* demethiolase STR3 controls the conversion of methionine into methanethiol. *Sci Rep-Uk* **6:** 21920.

Jia, K.Z., Zhu, L.W., Qu, X., Li, S., Shen, Y., Qi, Q., *et al*. (2019) Enzymatic *O*-glycosylation of etoposide aglycone by exploration of the substrate promiscuity for glycosyltransferases. *ACS Synth Biol* **8:** 2718–2725.

Kagkli, D.M., Bonnarme, P., Neuveglise, C., Cogan, T.M., and Casaregola, S. (2006) L-methionine degradation pathway in *Kluyveromyces lactis*: Identification and functional analysis of the genes encoding L-methionine aminotransferase. *Appl Environ Microbiol* **72:** 3330–3335.

Landaud, S., Helinck, S., and Bonnarme, P. (2008) Formation of volatile sulfur compounds and metabolism of methionine and other sulfur compounds in fermented food. *Appl Microbiol Biotechnol* **77:** 1191–1205.

Liu, J., Wu, Q., Wang, P., Lin, H., and Xu, Y. (2017) Synergistic effect in core microbiota associated with sulfur metabolism in spontaneous chinese liquor fermentation. *Appl Environ Microbiol* **83:** e01475–e1517.

Mansour, S., Beckerich, J.M., and Bonnarme, P. (2008) Lactate and amino acid catabolism in the cheese-ripening yeast *Yarrowia lipolytica*. *Appl Environ Microbiol* **74:** 6505–6512.

Mardones, W., Villarroel, C.A., Krogerus, K., Tapia, S.M., Urbina, K., Oporto, C.I., *et al*. (2020) Molecular profiling of beer wort fermentation diversity across natural *Saccharomyces eubayanus* isolates. *Microb Biotechnol* **13:** 1012–1025.

Martinez-Cuesta, M.D., Pelaez, C., and Requena, T. (2013) Methionine metabolism: major pathways and enzymes involved and strategies for control and diversification of volatile sulfur compounds in cheese. *Crit Rev Food Sci* **53:** 366–385.

McAuliffe, O., Kilcawley, K., and Stefanovic, E. (2019) Symposium review: Genomic investigations of flavor formation by dairy microbiota. *J Dairy Sci* **102:** 909–922.

Messerschmidt, A., Worbs, M., Steegborn, C., Wahl, M.C., Huber, R., Laber, B., and Clausen, T. (2003) Determinants of enzymatic specificity in the cys-met-metabolism PLP-dependent enzymes family: crystal structure of cystathionine γ-lyase from yeast and intrafamiliar structure comparison. *Biol Chem* **384:** 376–386.

Mura, C., McCrimmon, C., Vertrees, J., and Sawaya, M. (2010) An introduction to biomolecular graphics. *PLoS Comput Biol* **6:** e1000918.

Pal, G., Fong, S.Y., Kossiakoff, A.A., and Sidhu, S.S. (2005) Alternative views of functional protein binding epitopes obtained by combinatorial shotgun scanning mutagenesis. *Protein Sci*. **14:** 2405–2413.

Perea-Sanz, L., Peris, D., Belloch, C., and Flores, M. (2019) *Debaryomyces hansenii* metabolism of sulfur amino acids as precursors of volatile sulfur compounds of interest in meat products. *J Agric Food Chem* **67:** 9335–9343.

Perpete, P., Duthoit, O., Maeyer, S.D., Imray, L., Lawton, A.I., Stavropoulos, K.E., *et al*. (2005) Methionine catabolism in *Saccharomyces cerevisiae*. *FEMS Yeast Res* **6:** 48–56.

Sales, A., Paulino, B.N., Pastore, G.M., and Bicas, J.L. (2018) Biogeneration of aroma compounds. *Curr Opin Food Sci* **19:** 77–84.

Sha, S., Chen, S., Qian, M., Wang, C., and Xu, Y. (2017) Characterization of the typical potent odorants in Chinese roasted sesame-like flavor type liquor by headspace solid phase microextraction-aroma extract dilution analysis, with special emphasis on sulfur-containing odorants. *J Agric Food Chem* **65:** 123–131.

Sidhu, S.S., and Kossiakoff, A.A. (2007) Exploring and designing protein function with restricted diversity. *Curr Opin Chem Biol* **11:** 347–354.

Splivallo, R., Ottonello, S., Mello, A., and Karlovsky, P. (2011) Truffle volatiles: from chemical ecology to aroma biosynthesis. *New Phytol* **189:** 688–699.

Stone, E., Paley, O., Hu, J., Ekerdt, B., Cheung, N.K., and Georgiou, G. (2012) *De Novo* engineering of a human cystathionine-γ-lyase for systemic L-methionine depletion cancer therapy. *ACS Chem Biol* **7:** 1822–1829.

Sumbalova, L., Stourac, J., Martinek, T., Bednar, D., and Damborsky, J. (2018) HotSpot Wizard 3.0: web server for automated design of mutations and smart libraries based on sequence input information. *Nucleic Acids Res* **46:** W356–W362.

Sun, X., Yang, Z., Li, S., Tan, Y., Zhang, N., Wang, X., *et al*. (2003) *In vivo* efficacy of recombinant methioninase is enhanced by the combination of polyethylene glycol conjugation and pyridoxal 5′-phosphate supplementation. *Cancer Res* **63:** 8377–8383.

Weiss, G.A., Watanabe, C.K., Zhong, A., Godadard, A., and Sidhu, S.S. (2000) Rapid mapping of protein functional epitopes by combinatorial alanine scanning. *Proc Natl Acad Sci USA* **97:** 8950–8954.

Xu, Y.H., Jia, K.Z., and Tang, Y.J. (2018) Regulatory networks governing methionine catabolism into volatile organic sulfur-containing compounds in *Clonostachys rosea*. *Appl Environ Microbiol* **84:** e01840–e1918.

Yamagata, S., D'Andrea, R.J., Fujisaki, S., Isaji, M., and Nakamura, K. (1993) Cloning and bacterial expression of the *CYS3* gene encoding cystathionine γ-lyase of *Saccharomyces cerevisiae* and the physicochemical and enzymatic properties of the protein. *J Bacteriol* **175:** 4800–4808.

Yan, W., Stone, E., and Zhang, Y.J. (2017) Structural snapshots of an engineered cystathionine-γ-lyase reveal the critical role of electrostatic interactions in the active site. *Biochemistry* **56:** 876–885.

Supporting information

Additional supporting information may be found online in the Supporting Information section at the end of the article.

Supplementary Material

